Mathematical Model of the *Drosophila* Circadian Clock: Loop Regulation and Transcriptional Integration

Hassan M. Fathallah-Shaykh,[†‡*] Jerry L. Bona,[‡] and Sebastian Kadener[§¶]

[†]The University of Alabama at Birmingham, Departments of Neurology, Mathematics, Cell Biology, and Biomedical Engineering, The UAB Comprehensive Neuroscience Center, Birmingham, Alabama; [‡]The University of Illinois at Chicago, Department of Mathematics, Statistics, and Computer Science, Chicago, Illinois; [§]Brandeis University, Department of Biology, Waltham, Massachusetts; and [¶]The Hebrew University of Jerusalem, The Alexander Silberman Institute of Life Sciences, The Department of Biological Chemistry, Edmond J. Safra Campus, Givat-Ram, Jerusalem, Israel

ABSTRACT Eukaryotic circadian clocks include interconnected positive and negative feedback loops. The clock-cycle dimer (CLK-CYC) and its homolog, CLK-BMAL1, are key transcriptional activators of central components of the *Drosophila* and mammalian circadian networks, respectively. In *Drosophila*, negative loops include period-timeless and vrille; positive loops include par domain protein 1. Clockwork orange (CWO) is a recently discovered negative transcription factor with unusual effects on period, timeless, vrille, and par domain protein 1. To understand the actions of this protein, we introduced a new system of ordinary differential equations to model regulatory networks. The model is faithful in the sense that it replicates biological observations. CWO loop actions elevate CLK-CYC; the transcription of direct targets responds by integrating opposing signals from CWO and CLK-CYC. Loop regulation and integration of opposite transcriptional signals appear to be central mechanisms as they also explain paradoxical effects of period gain-of-function and null mutations.

INTRODUCTION

Circadian clocks exhibit 24-h behavioral and transcriptional oscillations. These oscillations are generated by interconnected transcriptional feedback loops. In particular, the *Drosophila* circadian clock has one positive and two negative loops that interconnect at CLK-CYC, a heterodimer of the clock (CLK) and cycle (CYC) proteins. CLK-CYC binds canonical E-box sequences to activate the transcription of direct targets clockwork orange (*cwo*), period (*per*), timeless (*tim*), vrille (*vri*), and par domain protein 1 (*Pdp1*, Fig. 1 *a*) (1–6). Clockwork orange (CWO) is a recently defined negative transcriptional regulator that directly targets the same genes as CLK-CYC (Fig. 1 *a*). The presence of circadianly expressed *cwo* orthologs in mouse (*dec1* and *dec2*) suggests that a similar feedback mechanism exists in mammals (7); this view may also extend to other animal systems (8).

Because CWO represses the transcription of *cwo*, *per*, *tim*, *vri*, and *Pdp1*, one expects *cwo* mutants to exhibit higher peak levels of all direct-target mRNAs compared to wild-type flies (wt). Both Matsumoto et al. (9) and Richier et al. (10) show that the peak levels of *per*, *tim*, *Pdp1*, and *vri* are lower in *cwo*-mutant flies compared to wt flies. Lim et al. also show that the peak levels of *per*, *Pdp1*, and *vri* are lower in *cwo*-mutant flies than in wt flies (the peak level of *tim* was not studied) (11). The results of Kadener et al. are consistent with those above, except in the case of *Pdp1* (8). The reasons why a *cwo* null mutation has these unusual effects on direct target genes are not known.

Glossop et al. described two negative interlocked feedback loops within the *Drosophila* circadian oscillator: 1), a per/tim loop that is activated by CLK-CYC and repressed by the period-timeless (PER-TIM) dimer; and 2), the vri/clk loop, consisting of the CLK-CYC heterodimer activating VRI, which represses *clk* transcription (6,12–14). The Pdp1/clk positive loop, which also interconnects at CLK-CYC, includes PDP1 acting as a transcriptional activator of *clk* mRNA (Fig. 1 *b*) (15–17). PER-TIM represses the transcriptional ability of CLK-CYC by inhibiting its DNA binding activity (18–21); furthermore, double-time (DBT) kinase appears to mediate these effects on CLK-CYC by phosphorylating PER and CLK (22–24). DBT is incorporated in our model as a positive and necessary regulator of the PER-TIM dimer.

Mathematical models of the circadian clock typically use the Michaelis-Menten and Hill-type equations, which require several parameters to model a single regulatory reaction. Furthermore, several equations are needed to model the ability of a molecule to regulate the state of another (15–17, 25–28). Here, we introduce a new system of nonlinear ordinary differential equations that model regulatory networks such that regulatory weights are represented by single parameters. The system is generic in the sense that it is applicable to mRNA, protein, protein dimer formation, or protein phosphorylation. We construct a new mathematical model of the *Drosophila* circadian clock and demonstrate that it is faithful in the sense that it replicates biological results. The model is then applied to study the regulatory effects of CWO and to suggest a resolution of the paradox of the effects of CWO on direct target genes. The model predicts that the actions of CWO on the interconnected loops elevate the level of

Submitted March 18, 2009, and accepted for publication August 12, 2009.

*Correspondence: hfathall@uab.edu

Editor: Arthur Sherman.

0006-3495/09/11/2399/10 $2.00

doi: 10.1016/j.bpj.2009.08.018

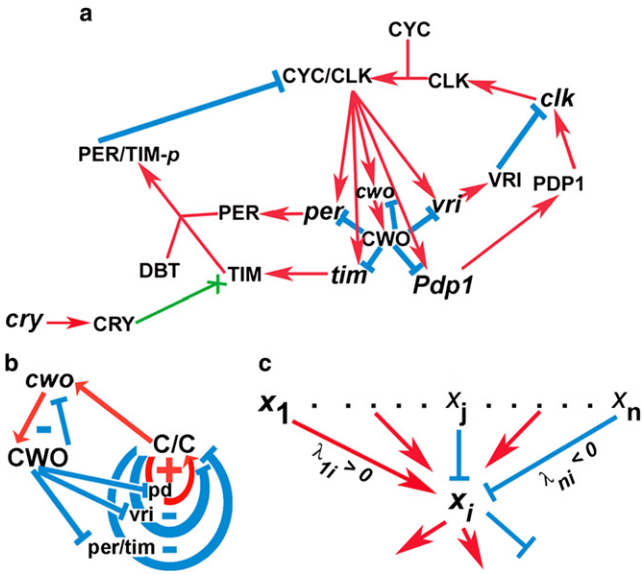

FIGURE 1 The network of the *Drosophila* circadian clock. (*a*) Cartoon depicting the *Drosophila* circadian molecular network; protein and mRNA are represented by capital letters and lower case, respectively. Red arrows and cyan lines indicate stimulatory and inhibitory interactions, respectively. The green arrow ending in X indicates that CRY protein enhances the degradation of TIM. The amounts of CYC and DBT are assumed to be constant. (*b*) Loop diagram of the network showing the CWO autorepressive loop (*cwo*, CWO), the per/tim and vri negative loops, and the Pdp1 (*pd*) positive loop. (*c*) Cartoon depicting a hypothetical example of molecules x_j, where $1 \le j \le n$, regulating the state of molecule x_i by positive (*red arrows*) or negative (*cyan lines*) interactions. Positive and negative real parameters are regulatory weights that simulate stimulation and repression, respectively (see Eq. 1).

CLK-CYC; the latter generates positive transcriptional signals on *per*, *tim*, *vri*, and *Pdp1* that outweigh the direct repressive actions of CWO. In the Results section, using the regulatory weights introduced by the new system of differential equations, we suggest a method for quantifying transcriptional signals. These ideas are applied to analyze simulations of *per* gain-of-function and null mutations.

METHODS

Numerical computations

Simulations are performed in MATLAB (The MathWorks, Natick, MA); the system of ordinary differential equations is solved numerically by the subroutine "ode45" (see the Supporting Material for MATLAB functions).

RESULTS

Interconnected positive and negative loops

A loop $(a_1,\ldots,a_n)$ is a sequence of interacting molecules such that 1), each of its molecules is figured only once; 2), for $1 < k \le n$, a_{k-1} is the only molecule that directly regulates a_k (either negatively or positively); and 3), a_n regulates a_1 (either negatively or positively). A loop is positive if it contains an even number of negative regulations, including zero, and is negative otherwise. For example, the loops (CYC-CLK, *Pdp1*, PDP1, *clk*, CLK) and (CYC-CLK, *vri*, VRI, *clk*, CLK) are positive and negative, respectively (Fig. 1 *a*).

The network shown in Fig. 1 *a* can be reduced to the loop diagram shown in Fig. 1 *b*, which includes three main loops that intersect at CLK-CYC. These are the (CLK-CYC, *per*/*tim*, PER-TIM, PER/TIM-p) and (CLK-CYC, *vri*, VRI, *clk*, CLK) negative loops and the (CLK-CYC, *Pdp1*, PDP1, *clk*, CLK) positive loop. Henceforth, we will refer to these loops as per/tim, vri, and Pdp1 loops, respectively. The network also includes a negative auto-repressive loop (*cwo*, CWO); notice that this negative loop, which includes two molecules, *cwo* and CWO, doesn't interconnect at CLK-CYC. Recall that CLK-CYC binds to E-box sequences leading to transcriptional activation of direct targets, including *cwo*. The CWO protein specifically binds and represses the promoter elements/E-box sequences of direct targets, including *cwo* (9,11).

System of ordinary differential equations

We introduce a nonlinear, autonomous, first-order system of ordinary differential equations (Fig. 1 *c*). Assuming that genes/proteins $j \in \{1,\ldots, n\}$ regulate the production of gene/protein i, we use the following type of differential equations as a general model:

$$\frac{dx_i(t)}{dt} = \rho_i g\left(\sum_{j=1}^{n} \lambda_{ji} x_j(t) - \delta_i x_i(t)\right) x_i(t)(s_i - x_i(t)), \quad 1 \le j \le n, \tag{1}$$

where x_i is the state vector representing the concentration of molecule i at its site of action. The real parameters, λ_{ji}, are regulatory weights that encode the effects of molecule j on the production rate of molecule i. Positive and negative λ_{ji} are interpreted as j activating or repressing, respectively, molecule i. The absolute value of λ_{ji} reflects the strength of stimulation or repression. Notice that λ_{ji} is applicable to several biochemical reactions, such as the formation of a protein dimer (i.e., CLK-CYC), the effects of a kinase (i.e., DBT), the effects of a transcription factor on a promoter (i.e., the effect of CLK-CYC or CWO on direct target genes), and mRNA translation to protein (i.e., PER or TIM).

The sum of the regulatory influences is modulated by an odd sigmoid function, $g : \mathbb{R} \to \mathbb{R}$, of the form

$$g(u) = \frac{u}{\sqrt{1 + u^2}} = \tanh\left(\ln\left(u + \sqrt{1 + u^2}\right)\right),$$

together with a real parameter $\rho_i > 0$ that indicates the maximum rate of formation of i. The model incorporates logistic terms $((x_i)(s_i - x_i))$, where constants $s_i \ge 0$ indicate the saturation level of molecule i. The real parameter δ_i is the decay rate of i. Notice also that because x_i denotes the concentration of molecule i at the site of its action, the

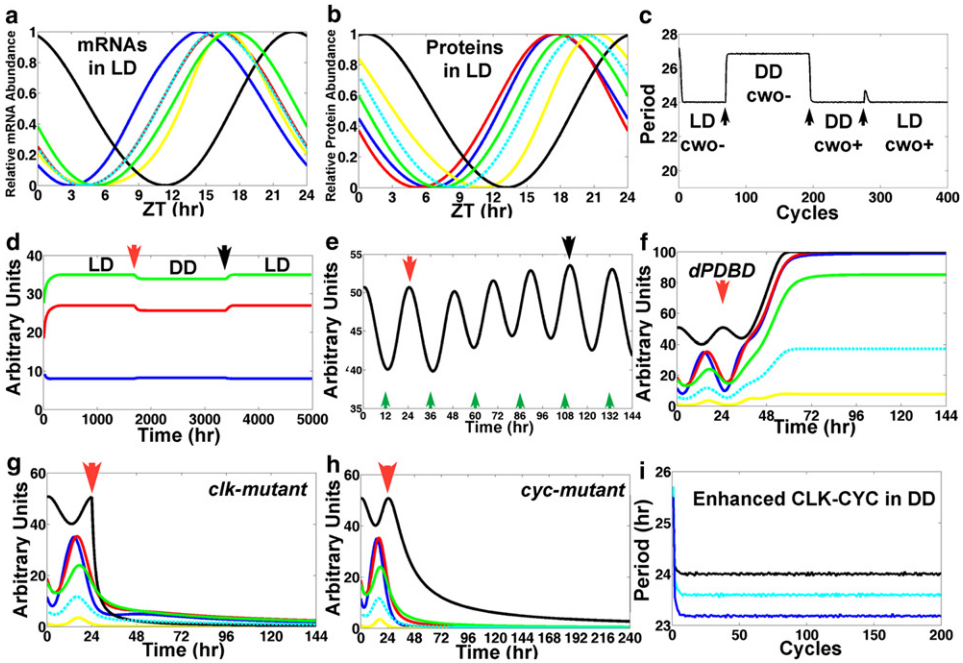

FIGURE 2 The model replicates biological results. (*a*) Plot of the results of model simulations in LD of the concentrations of *clk* (*black*; peak, 22.8 h), *per* (*blue*; peak, 14.4 h), *tim* (*red*; peak, 16.1 h), *cwo* (*yellow*; peak, 16.8 h), *Pdp1* (*green*; peak, 17.4 h), and *vri* (*cyan*; peak, 15.9 h). (*b*) Plot of the results of model simulations in LD of the concentration of the CLK (*black*; peak, 0.7 h), PER (*blue*; peak, 17.7 h), TIM (*red*; peak, 17.6 h), CWO (*yellow*; peak, 21.2 h), PDP1 (*green*; peak, 19 h), and VRI (*cyan*; peak, 20 h). Relative abundance is determined by $(x - \min)/(\max - \min)$. The Zeitgeber reference time is described in LD conditions only. To define a time reference in DD conditions we set time 0 at −0.7 h of the peak of the CLK protein so that the latter peaks at the same time in both LD and DD. The peak times of the direct-target genes and proteins in DD are as given in *a* except for TIM, which peaks at 16.6 h. (*c*) Plot of the period (time between the peaks of *per* mRNA) in an experiment where the model cycles first in LD with *cwo* mutation (cwo−), then in DD with *cwo* mutation, then in DD with wt *cwo* (cwo+), and finally in LD with wt *cwo*. Transitions are applied at ZT = 0 (*arrows*). Notice the minimum variability of the 24-h period in both DD and LD in wt *cwo* simulations. (*d*) Plot of the peak (*green*) and trough (*blue*) levels and the amplitude (peak − trough, *red*) of *per* mRNA, computed from an experiment where the model cycles first in LD (0 to *red arrow*), then in DD (*red arrow* to *black arrow*), and finally in LD. Transitions from LD to DD and from DD to LD are applied at ZT = 0. (*e*) The model clock resets (*black arrow*) 4.5 days after a shift of +12 h is applied at the red arrow. Notice that CLK evolves to a peak around midnight of the previous time zone (*black arrow*). Green arrows point to ZT = 12 h of the previous time zone. (*f–h*) Plots of the simulated dynamics of dPDBD (in DD) (*f*), *clk* (in LD) (*g*), and *cyc* (in DD) (*h*) null mutations applied at time = 24 h (*red arrows*). Notice the elevated and constant levels of *per* (*blue*) and *tim* (*red*) mRNAs in simulated dPDBD mutants and the low levels of *per* and *tim* mRNAs in *clk*- and *cyc*-null mutants. The mRNA levels of *per*, *tim*, *cwo*, *Pdp1*, and *vri* are shown in blue, red, yellow, green, and cyan, respectively. The CLK protein is shown in black. (*i*) Plot of the period of the wt model (*black*) and the simulations where all the positive regulatory weights of CLK-CYC on direct-target genes are increased by 15% (*cyan*) or 30% (*blue*) in DD conditions.

parameters model not only direct stimulation or repression, but also the cumulative effects of transport and diffusion across cellular compartments. The actual equations and parameters are provided in MATLAB functions and pdf copies in the Supporting Material.

Parameters and simulations

The parameters are optimized to yield a numerical solution such that the clock oscillates with a 24-h period both in light-dark (LD) and dark-dark (DD) cycles indefinitely and with timely peaks of direct targets (see Fig. 2, *a–c*, and Supporting Material). The period exhibits minimum variations, and the amplitudes are effectively constant; in particular, the period ranges from 23.9718 h to 24.0292 h in LD and from 23.9633 h to 24.0483 h in DD conditions (Fig. 2 *d*). CRY is a light-regulated cryptochrome that leads TIM to its subsequent degradation. To account for different photoperiods (i.e., LD), the model uses oscillations of *cry* mRNA obtained from published microarray expression data (see Fig. S1 in the Supporting Material) (8). The *cry* mRNA oscillations, approximated by fitting with linear elements, keep the Zeitgeber time (ZT; i.e., time mod(24) in LD). DD conditions are simulated by annulling the effects of CRY on TIM (i.e., $\lambda_{CRY,\,TIM} = 0$).

The timing of the peaks of the oscillating direct-target mRNAs and proteins is consistent with biological observations (Fig. 2, *a* and *b*). In particular, the model predicts that *per*, *tim*, PER, and TIM peak at ZT = 14.4, 16.1, 17.7, and 17.6 h, respectively, in LD. These results are within range of published results for *per* (13–16 h), *tim* (13–16 h), PER (18–20 h), and TIM (17–18 h). The predicted times of the peak of CLK (0.7 h) and the period between the peaks of *clk* and CLK (1.9 h) are also within range of those in the literature (1,8,10,29–34). The oscillations of mRNAs and proteins in DD have the same phases as in LD conditions except for the TIM protein, which peaks 1 h earlier in DD (16.6 h versus 17.6 h).

The model replicates biological observations

Once the model was established as described in the previous section, the next step was to test whether it could predict the effects of unfitted perturbations. A major characteristic of the circadian clock is its capacity to respond to different time zones. TIM degradation is the main response of the clock to light; this effect is mediated by CRY (Fig. 1 *a*) (35,36). We study the response of the model to a 12-h time shift (simulating the effects of time-zone changes in LD). This

is done by advancing the level of *cry* mRNA at ZT = 0 to its level at ZT = 12 h (i.e., LD, DL, DL,…). The outcome of the numerical experiment is that the molecular clock is reentrainable by light, i.e., the CLK protein evolves smoothly from peaking at ZT = 12 h, which is ZT = 0 h in the previous time zone, to peaking at ZT = 0 h in the new time zone, although the transition takes 4.5 days to complete (see Fig. 2 *e*). This entrainment is valid for all mRNAs. These results are in concordance with the behavior of the mammalian clock in response to shifting the light/dark cycle by 12 h (LD to DL); Chen et al. showed near-complete phase reversal (11.55 h) of behavioral and molecular phase shifts after 5 days of DL (37).

We next tested whether or not the model can predict accurately the molecular effects of mutations in the core clock components. Null mutations are simulated by setting the appropriate $\lambda_{ji} = 0$. For example, *clk* mutations are simulated by setting $\lambda_{clk,\ CLK} = 0$. A mutation of the DBT binding domain on PER (dPDBD) is simulated by $\lambda_{\mathrm{DBT,\ PER/TIM\text{-}p}} = 0$. Fig. 2 *f* plots a simulation of the dPDBD mutation in DD, showing the absence of oscillations with elevated levels of *per* and *tim* mRNA. These results are largely consistent with biological data for dPDBD from the literature, which are arrhythmic with elevated PER and TIM (23,38–40). Furthermore, simulations of *cyc*- and *clk*-mutant flies are also consistent with biological data showing that the mutant flies are arrhythmic with low levels of PER and TIM (Fig. 2, *g–h*) (1,5).

Kadener et al. analyzed the effects of enhancing the activity of the CLK-CYC by generating CYC-VP16, a well studied construct that imparts strongly enhanced activity of the CLK-CYC-VP16 complex (41). This experimental design is simulated by increasing the positive regulatory effects of CLK-CYC on direct-target genes. The model replicates the biological outcome by yielding a higher peak level of *per* mRNA (data not shown) and a shorter period in DD (Fig. 2 *i*). The ability of the model system to replicate biological results for which it was not fit gives a certain level of confidence in its overall faithfulness. The results of simulations of *per*-null and gain-of-function mutations are discussed below.

Modeling the actions of CWO

With the aim of understanding the role of CWO in the circadian molecular network, we instituted in silico *cwo*-null mutations. Consistent with biological data, mutations in this gene lead to low mRNA peak levels of *per*, *tim*, *vri*, and *Pdp1* in both LD and DD conditions. It is interesting to note that the model also predicts that, as compared to wt RNA, the peak level of *cwo* mRNA is higher in the *cwo*-mutant model in both LD and DD conditions (see Fig. S2 and Fig. S3). The model predicts a period of 26.8 h in *cwo*-mutants in DD conditions (Fig. 2 *c*). These results are consistent with biology, since the experimentally measured period is ~26.5 h (8,10). Furthermore, as in biological observations, the *cwo*-mutant model yields a period of 24 h in LD conditions. This satisfactory outcome further enhances our confidence in the model.

Direct-target genes receive two opposing signals, a direct stimulus from CLK-CYC and a direct repressive action by CWO (see Fig. 1 *a*). In addition, CWO regulates the level of the CYC-CLK, presumably through its actions on each of three main loops (i.e., the per/tim and vri negative loops and the Pdp1 positive loop (Fig. 1 *b*)). It is therefore uncertain how the absence of CWO affects direct-target genes. We hypothesized that the behavior of the network may be deduced from its loop structure.

CWO is a loop regulator

The in silico experiments detailed in this section are performed to elucidate the mechanism of CWO action. Recall that in addition to its autorepressive effects, CWO has three repressive loop actions at 1), the per/tim negative loop, 2), the vri negative loop, and 3), the Pdp1 positive loop (Fig. 1 *b*). To optimize the presentation, the experiment begins from a baseline absence of any CWO function (i.e., mutant *cwo* (Fig. 3, *black line*)), then proceeds by turning on either single or combinations of repressive actions of CWO in DD conditions. Figs. 3 and 4 plot the mRNA levels of the direct-target genes as well as that of CLK-CYC in response to the targeted parameter perturbations; each panel represents a molecule and the results of the experiments are shown in color. It can be intuited that repressing a single positive or negative loop would yield lower and higher peak levels of CLK-CYC, respectively.

Starting from a baseline of no CWO action, then selectively turning on the CWO autorepression, causes the peak level of *cwo* mRNA to decrease (Fig. 3 *a*, *black* versus *red*), but the mRNA peak levels of the other direct target genes remain unchanged (Fig. 3, *b–f*). This is expected, because this configuration isolates the (*cwo*, CWO) autorepressive loop from the other components of the clock (Fig. 1 *b*). Next, we turn on two repressive actions:1), the CWO autorepression, and 2), one of either the Pdp1 (positive), vri (negative), or per/tim (negative) loops. The results confirm that downregulating a positive or a negative loop lowers (Fig. 3, *red* to *yellow*) and elevates (Fig. 3, *red* to *cyan* or *red* to *magenta*), respectively, the peaks of the CYC/CLK dimer and all direct-target genes.

Next, we turn on three CWO-mediated repressive actions, namely 1), the CWO autorepression; 2), repression of the Pdp1 positive loop; and 3), repression of either the vri or the per/tim negative loops (Fig. 4). It is interesting that downregulating the per/tim negative loop is more effective than downregulating the vri loop in elevating the peak levels (Fig. 4, *yellow* to *green* versus *yellow* to *red*), suggesting that the per/tim negative loop is more repressive than the vri negative loop. The results provide a confirmation of the idea that repression of a positive or a negative loop by a

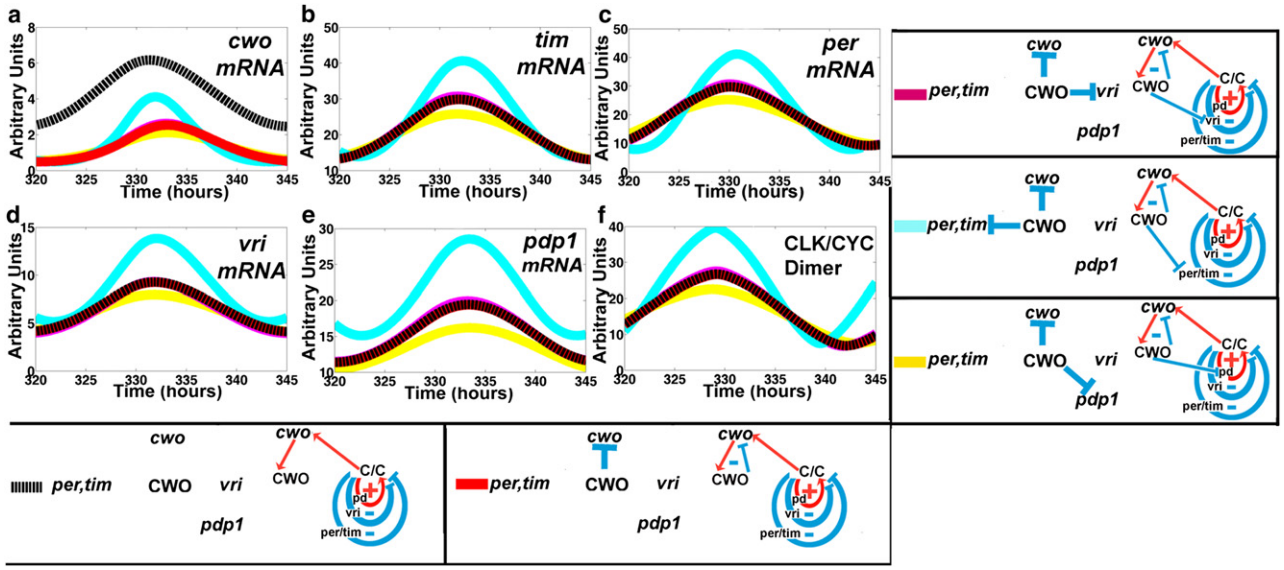

FIGURE 3 Actions of CWO on the loops. (*a–f*) mRNA concentrations of *cwo*, *tim*, *per*, *vri*, *pdp1*, and CLK-CYC in response to selective activation of the repressive actions of CWO in DD conditions. Dotted black lines represent the mutant model. The red line denotes the selective activation of the CWO autorepressive loop (*cwo*, CWO) only. Magenta, cyan, and yellow lines indicate the activation of two repressive actions, the CWO autorepressive loop plus one of either the vri or per/tim negative loops, or the Pdp1 positive loop (*pd*), respectively.

molecule located outside the loop (i.e., CWO) causes negative and positive effects, respectively, on the elements of the loop.

Actions of CWO on direct targets

The next experiments are done to understand the cumulative effects of CWO on the three loops that interconnect at CLK-CYC in LD and DD conditions (see Fig. S4 and Fig. S5). Specifically, we start from the baseline, where CWO selectively represses its own transcription (Fig. S4 and Fig. S5, *red*), and turn on all three loop-repressive actions of CWO (i.e., the wt model (Fig. S4 and Fig. S5, *blue*)). The results reveal that the peak levels of CLK-CYC are higher in the wt than in the *cwo*-mutant model (Fig. S4 *f* and Fig. S5 *f*, *red* to *blue*). Recall that each direct-target gene receives positive and negative transcriptional stimuli from CLK-CYC and CWO, respectively. Notice that the increase in CLK-CYC

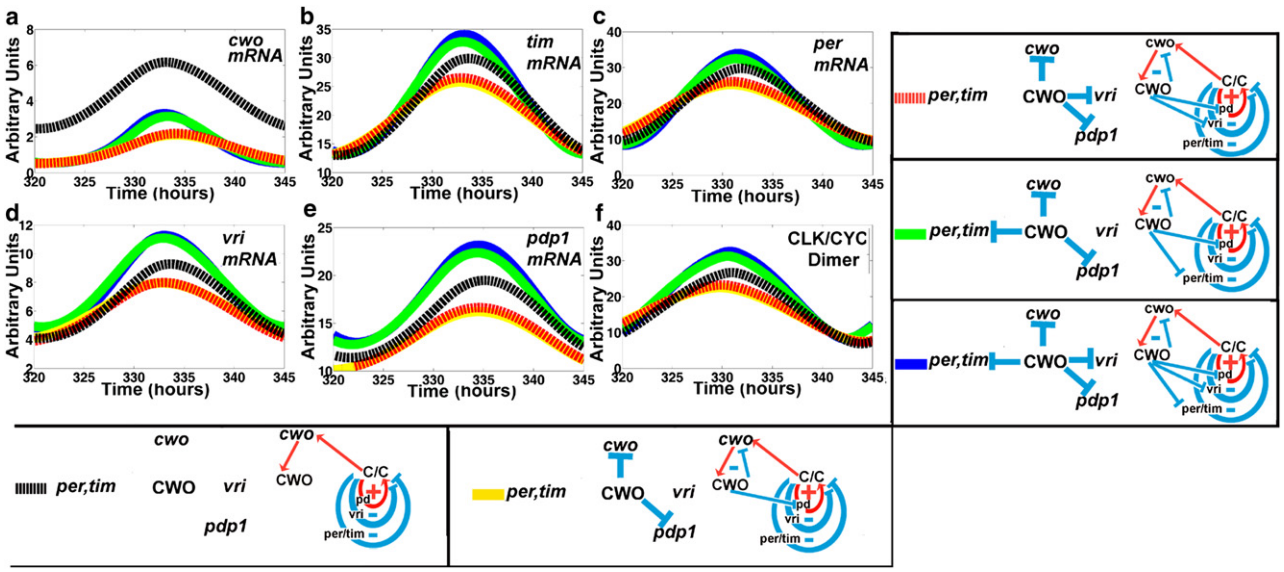

FIGURE 4 CWO regulates the loops. (*a–f*) mRNA concentrations of *cwo*, *tim*, *per*, *vri*, *pdp1*, and CLK-CYC in response to selective activation of the repressive actions of CWO in DD conditions. Blue and black lines represent the wt and mutant models, respectively. The yellow line denotes the selective activation of the CWO autorepressive loop (*cwo*, CWO) and the Pdp1 positive loop (*pd*). Red and green lines denote the activation of three CWO-repressive actions, the CWO autorepressive loop plus the Pdp1 positive loop plus one of either the vri (*red*) or the per/tim (*green*) negative loops, respectively.

(referred to as $\Delta x_{C/C} = x_{C/C} - x_{C/C}^{cwo\text{-}mutant}$) causes a positive effect on the transcription of *per*, *tim*, *vri*, and *Pdp1*, despite the repressive effects of CWO (*blue* versus *red*). This suggests that the positive effects of $\Delta x_{C/C}$ outweigh the repressive actions of CWO on the transcription of *per*, *tim*, *vri*, and *Pdp1*.

To understand how *cwo* integrates the opposing transcriptional effects of $\Delta x_{C/C}$ and CWO, we examine the models of 1), null-mutant *cwo* (i.e., no CWO actions (Fig. S4 and Fig. S5 *a*, *black dotted line*); 2), *cwo* acted on by CWO only (Fig. S4, and Fig. S5 *a*, *red*); and 3), *cwo* acted on by both CWO and $\Delta x_{C/C}$ (wt model, Fig. S5 *a*, *blue*). The results reveal that the positive transcriptional effects of $\Delta x_{C/C}$ partially reverse the repressive effects of CWO because they elevate the transcription of *cwo* (*blue* versus *red*) but not to the level seen in the mutant *cwo* model (*blue* versus *dotted black*). These findings suggest that unlike the other direct-target genes, the outcome of the opposing transcriptional actions of $\Delta x_{C/C}$ and CWO at *cwo* favors repression.

Modeling the integration of opposing transcriptional signals

Our next goal is to elucidate the law that governs the integration of the opposing transcriptional effects of $\Delta x_{C/C}$ and CWO on a direct-target gene (g) at the time of its peak (t_g). We examine 1), the ''wiring'' as reflected by the regulatory weights $\lambda_{C/C,\,g}$ and $\lambda_{CWO,\,g}$, and 2), $\Delta x_{C/C}$ and the concentration level of the CWO protein (x_{CWO}). Recall that the parameters $\lambda_{C/C,\,g}$ and $\lambda_{CWO,\,g}$ are positive and negative and that their absolute values reflect the strength/weight of transcriptional enhancement and repression, respectively. The difference between the peak concentrations of direct-target gene g in the wt and *cwo*-mutant models ($\Delta Y_g = Y_g - Y_g^{cwo\text{-}mutant}$) can be expressed as (see Supporting Material)

$$\mathrm{sign}(\Delta Y_g) = \mathrm{sign}\left[\Delta x_{C/C}(t_g)\lambda_{C/C,g} - x_{CWO}(t_g)\left|\lambda_{CWO,g}\right|\right]. \quad (2)$$

Hence, a transcriptional signal at the peak of a direct-target gene can be modeled by the product of the concentration of the transcriptional modulator (i.e., $\Delta x_{C/C}(t_g)$ or x_{CWO}) and the absolute values of the weights of the transcriptional regulation (i.e., $|(\lambda_{C/C,g})|$ or $|\lambda_{CWO,g}|$). Furthermore, the transcription of a direct-target gene at its peak is enhanced ($\Delta Y_g > 0$) or repressed ($\Delta Y_g < 0$) when the positive signal, $\Delta x_{C/C}(t_g)\lambda_{C/C,g}$, is larger or smaller, respectively, than the negative transcriptional signal, $[x_{CWO}(t_g)|\lambda_{CWO,g}|]$ (Fig. 5). We conclude that the integration of the actions of CWO on the loops causes an elevation of CLK-CYC ($\Delta x_{C/C} > 0$). In the wt model, each direct-target gene integrates a positive signal from $\Delta x_{C/C}$ and a negative signal from CWO. The peak levels of *tim*, *per*, *vri*, and *Pdp1* are higher in the wt than in the *cwo*-mutant model because the positive transcriptional signals outweigh the negative ones (i.e., $\Delta x_{C/C}(t_g)\ \lambda_{C/C,g} > x_{CWO}(t_g)|\lambda_{CWO,g}|$, Fig. 5). However, the transcription of *cwo* is repressed in the wt model because the negative transcriptional signal is dominant (i.e., $\Delta x_{C/C}(t_{cwo})\lambda_{C/C,cwo} < x_{CWO}(t_{cwo})|\lambda_{CWO,cwo}|$). The fact that the integration of transcriptional signals on direct targets was not considered when Eq. 1 was constructed gives additional confidence in its overall faithfulness.

To understand the effects of CWO on the period, we examine simulations where individual repressive weights of CWO are increased or decreased by 10% in DD conditions. Recall that by repressing *Pdp1*, *per*, *tim*, and *vri*, CWO acts on the loops that interconnect at CLK-CYC, namely, the Pdp1 positive loop and the per/tim and vri negative loops. The results reveal that perturbations that increase or decrease the level of CLK-CYC shorten and elongate the period, respectively (Fig. 6). Notice that these findings are consistent with the outcome of the simulation where the activity of CLK-CYC is enhanced (Fig. 2 *i*). In particular, by repressing *Pdp1*, CWO downregulates the activity of the Pdp1 positive loop in the sense that the level of CLK/CYC decreases. Similarly, by repressing *per* or *vri*, CWO downregulates the per/tim and vri negative loops as the levels of CLK-CYC increase. Thus, by repressing the transcriptional levels of *per*, *vri*, and *Pdp1*, CWO regulates the activity of the three main loops by making the positive loops ''less positive'' and the negative loops ''less negative.''

The results of the perturbation experiments also demonstrate that *per* mRNA reacts in the same direction as CLK-CYC (Fig. 6 *a*). However, it appears paradoxical that increasing the repressive activity of CWO on *per* elevates the level of *per* mRNA instead of suppressing it (Fig. 6).

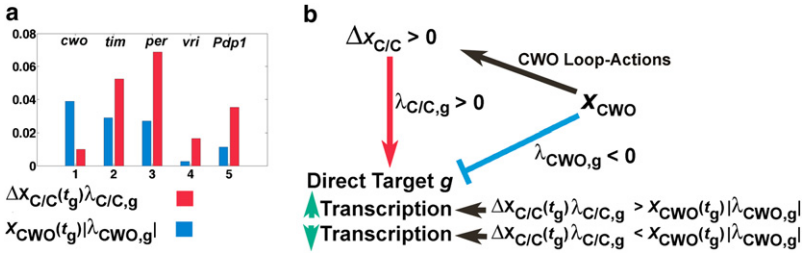

FIGURE 5 Integration of opposite transcriptional signals. (*a*) Bar plot of the absolute values of the positive ($\Delta x_{C/C}(t_g)\lambda_{C/C,g}$; *red*) and negative ($x_{CWO}(t_g)|\lambda_{CWO,g}|$; *blue*) transcriptional signals at the peak of each direct-target gene in the wt model in LD. (*b*) The cumulative effects of the actions of the CWO protein on the three loops cause an increase in peak levels of CLK-CYC ($\Delta x_{C/C} > 0$), which leads to higher peaks of *vri*, *Pdp1*, *per*, and *tim*, because the values of the positive signals are larger than those of the negative signals. The transcription of *cwo* is repressed because the negative signal is dominant. The term $x_{CWO}(t_g)$ refers to the concentration of CWO protein at the time of the peak of a direct-target gene.

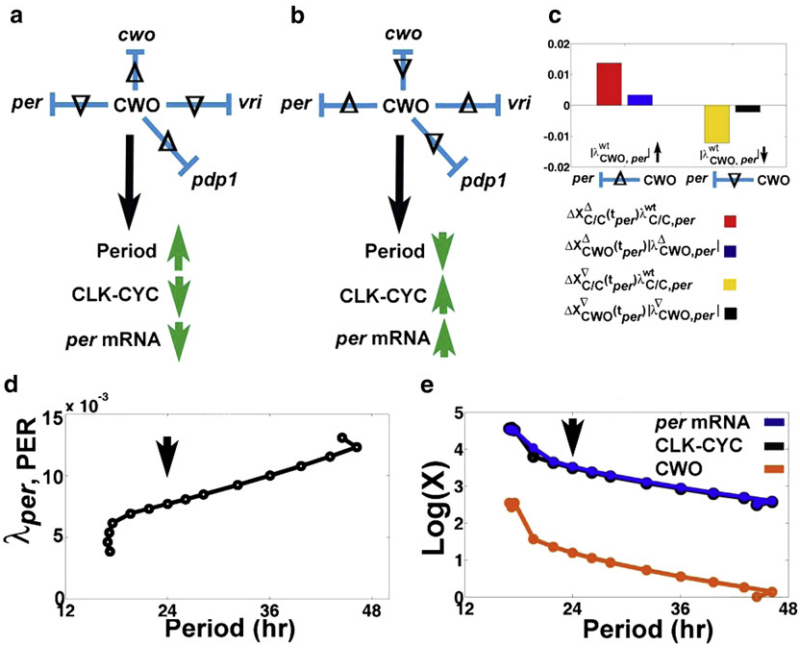

FIGURE 6 Effects of single repressive effects of CWO on the period in DD. (*a* and *b*) Summary of how the period and peak levels of CLK-CYC and *per* mRNA react in simulations where the absolute value of a single repressive regulatory weight of CWO is increased (Δ) or decreased (∇) by 10% in DD. Neither CLK-CYC nor the period is affected by similar perturbations of the repressive actions of CWO on *tim*. (*c*) Bar graph from an experiment where $|\lambda^{wt}_{CWO,per}|$ is increased ($|\lambda^{\Delta}_{CWO,per}|$) or decreased ($|\lambda^{\nabla}_{CWO,per}|$) by 10% in DD, leading to higher ($\Delta x^{\Delta}_{C/C}(t_{per}) > 0$ and $\Delta x^{\Delta}_{CWO}(t_{per}) > 0$) and lower ($\Delta x^{\nabla}_{C/C}(t_{per}) < 0$ and $\Delta x^{\nabla}_{CWO}(t_{per}) < 0$) levels of CLK-CYC and CWO, respectively. The symbol t_{per} refers to ZT at the peak of *per*. In the case of $\lambda^{\Delta}_{CWO,per}$, the positive transcriptional signal for *per* outweighs the negative one ($\Delta x^{\Delta}_{C/C}(t_{per})\lambda^{wt}_{C/C,per} > \Delta x^{\Delta}_{CWO}(t_{per})|\lambda^{\Delta}_{CWO,per}|$). In the case of $\lambda^{\nabla}_{CWO,per}$, the positive transcriptional signal for *per* is smaller than the negative one ($\Delta x^{\nabla}_{C/C}(t_{per})\lambda^{wt}_{C/C,per} < \Delta x^{\nabla}_{CWO}(t_{per})|\lambda^{\nabla}_{CWO,per}|$). (*d*) Response of the period to the titration of $\lambda_{per,\ PER}$. Notice the apparent linear relation in the interval $\lambda_{per,\ PER} \in [0.0069, 0.0123]$; $y = 2 \times 10^{-4} \times x + 0.0029$ (norm of residuals $= 2.7312 \times 10^{-4}$). (*e*) Based on the data plotted in *d*, and Plots of log(X) versus period, where *X* denotes the level of CLK-CYC (*black*), *per* (*blue*), or CWO (*orange*). The arrows in *d* and *e* indicate the wt model.

This paradox is easily resolved when we consider the idea of loop regulation and the method for integrating opposite transcriptional signals detailed in Fig. 5 (see Fig. 6 *c*). In particular, increasing the strength of CWO-mediated repression of the per/tim negative loop ($|\lambda^{\Delta}_{CWO,per}| > |\lambda^{wt}_{CWO,per}|$) elevates CLK-CYC, a positive regulator of CWO (i.e., $\Delta x^{\Delta}_{C/C}(t_{per}) > 0$ and $\Delta x^{\Delta}_{CWO}(t_{per}) > 0$). After integrating the two opposing signals, the peak level of *per* increases because the positive transcriptional signal ($\Delta x^{\Delta}_{C/C}(t_{per})\lambda^{wt}_{C/C,per}$) outweighs the negative one ($\Delta x^{\Delta}_{CWO}(t_{per})|\lambda^{\Delta}_{CWO,per}|$). In a similar way, decreasing the strength of the CWO-mediated repression of the per/tim negative loop (i.e., $|\lambda^{\nabla}_{CWO,per}| < |\lambda^{wt}_{CWO,per}|$) lowers both CLK-CYC and CWO (i.e., $\Delta x^{\nabla}_{C/C}(t_{per}) < 0$ and $\Delta x^{\nabla}_{CWO}(t_{per}) < 0$). However, the level of *per* decreases because the positive transcriptional signal ($\Delta x^{\nabla}_{C/C}\lambda^{wt}_{C/C,per}$) is smaller than the negative signal ($\Delta x^{\nabla}_{CWO}(t_{per})|\lambda^{\nabla}_{CWO,per}|$). Finally, the results highlight the usefulness of the regulatory network introduced in Eq. 1 in advancing our understanding of the complex actions of *cwo*, in simulating how the network integrates the actions of CWO on multiple loops, and in uncovering a method for integrating opposite transcriptional signals at each direct-target gene (Eq. 2).

Simulations of *per* mutations

Flies with chromosomal deletions of the *per* locus are arrhythmic (39,42). The per^{01} is a *per* mutation with an early stop codon corresponding to position 464 of the amino acid sequence (43). The levels of *per* mRNA are inversely correlated with period length, so that flies with the lowest levels of *per* have slow-running biological clocks (44,45). Based on these observations, Baylies et al. suggest that per^{01} is a null mutation (43). Notice that the perturbation experiments of Fig. 6, *a–c*, are consistent with the idea that low levels of *per* are associated with long periods. To investigate how the model reacts to *per* mutations, we titrate $\lambda_{per,\ PER}$ and examine the levels of *per*, CLK-CYC, and CWO, and the period in DD (Fig. 6 *d*). The results reveal an apparent linear correlation between $\lambda_{per,\ PER}$ and the period within bounds and confirm that *per* mRNA levels are inversely correlated to period length (Fig. 6, *d* and *e*). Nonetheless, our simulations suggest a conclusion different from that of Baylies et al. Specifically, the results of simulations of PER gain of function in LD and DD ($\lambda_{per,\ PER}$ is increased by 25%) reveal persistent oscillations of *per*, *tim*, and *cry* mRNAs with lower peaks compared to the wt model; the period is 24 h in LD (Fig. 7, *a* and *b*). The peak levels of both *per* and *tim* in LD and DD are at 78% and 57%, respectively, of the levels in the wt model (Fig. 7 *a*). In addition, *clk* shows minute oscillations close to the trough level of the wt model (Fig. 7 *a*). Simulations of PER gain of function in DD reveal further depression of the amplitudes leading to minute oscillations in *per*, *tim*, and *clk* (Fig. 7 *b*). These results in PER gain-of-function experiments are strikingly similar to the behavior of *per*, *tim*, and *clk* in per^{01} flies (2,29,32,38,39,43,46,47). Furthermore, simulation of a *per*-null mutation predicts that the clock is arrhythmic with elevated levels of *per* and *tim* (Fig. 7 *c*). If we assume that the network topology shown in Fig. 1 *a* is accurate, the model suggests that per^{01} could be a gain-of-function mutation rather than a null mutation in the sense that it leads to enhanced repression of CLK-CYC. The clock is arrhythmic in the *per*-null mutant model because all the eigenvalues of the flow matrix have negative real parts and only two have

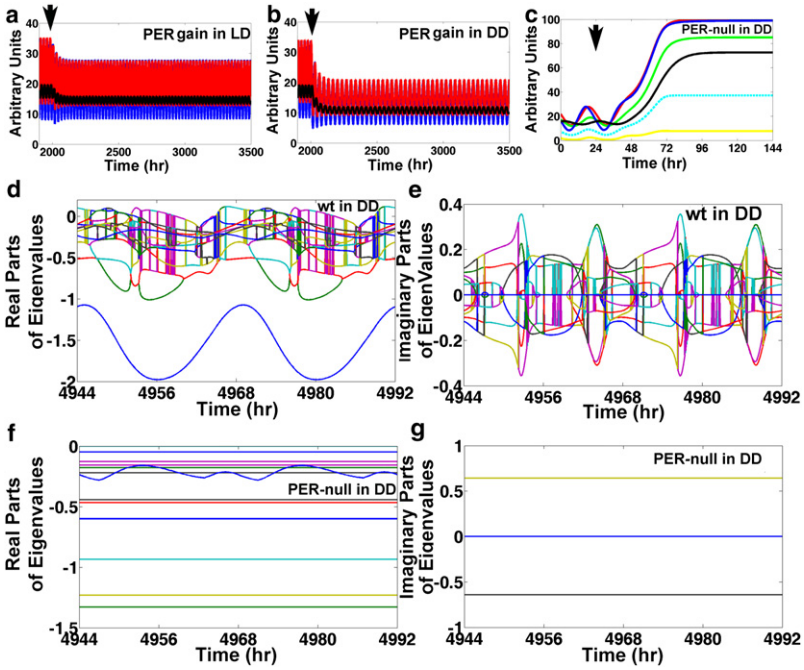

FIGURE 7 Simulations of PER gain and loss of function. (*a* and *b*) Reactions of *per* (*blue*), *tim* (*red*), and *clk* (*black*) mRNAs when $\lambda_{per,\ \mathrm{PER}}$ is increased by 25% (PER gain of function) at the arrows in LD and DD, respectively. (*c*) Results of a simulation where a *per*-null mutation ($\lambda_{per,\ \mathrm{PER}} = 0$) is applied at the arrow for *per* (*blue*), *tim* (*red*), *clk* (*black*), *cwo* (*yellow*), *vri* (*cyan*), and *Pdp1* (*green*) direct-target genes. (*d* and *e*) Real and imaginary parts, respectively, of the eigenvalues (*colored lines*) of the flow matrix of the wt model in DD; observe that the real parts cross the *x* axis. (*f* and *g*) Real and imaginary parts of the eigenvalues (*colored lines*) of the flow matrix of the *per*-null model in DD; all the real parts are negative and only two conjugate imaginary parts are nonzero. Notice that times 4944 h, 4968 h, and 4992 h correspond to ZT = 0 h, and times 4956 h and 4980 h correspond to ZT = 12 h.

nonzero conjugate and constant imaginary parts (see Fig. 7, *d*–*g*). The real and imaginary parts of the eigenvalues in the *cwo*-mutant model are shown in Fig. S6.

Comment

Sabhouri-Ghomi et al. have discussed some of the limitations of the Michaelis-Menten equations (48). The authors find that the Michaelis-Menten kinetics may be misleading in modeling protein interaction networks. A practical limitation of detailed kinetic reactions is that individual parameters don't all directly relate to measurable interactions within the network. We have been inspired by the gene circuits of Reinitz and colleagues (49–56). The system shown in Eq. 1 has several advantages, namely that its parameters model regulatory effects within the network and that it is generic in the sense that it is applicable to transcriptional, translational, as well as posttranslational mechanisms (57). In particular, the use of regulatory weights in Eq. 1 set the stage for Eq. 2, which models transcriptional signals and integration.

Loops are present in many molecular systems like the mammalian circadian clock, the cell cycle, NF-kB and p53 responses, calcium spikes, and the sinoatrial pacemaker. Negative feedback aligns dose responses and the design of positive-plus-negative feedback achieves a widely tunable frequency and stable amplitudes (58,59). The network of the *Drosophila* clock includes interconnected positive and negative loops. The network model shown in Fig. 1 replicates a range of outcomes, including oscillations with a 24-h period, timely peaks, and entrainment in response to time shifts, and it reacts in harmony with the results of experimental mutations and perturbations (Fig. 2). The findings uncover the principle that large molecular networks may be reduced to a few positive and negative loops (see Fig. 1). In fact, the results demonstrate that the dynamical behavior of the whole system can be predicted by simple rules, such as suppressing negative and positive loops leads to positive and negative effects, respectively (see Figs. 3 and 4).

Transcription is a dynamic process that involves continuous tuning of mRNA production in response to opposing signals. Equation 2 quantifies transcriptional signals and the integration of opposite signals. The idea that transcription reacts in harmony with the outcome of weighing opposite signals is intuitive. The fact that such a relatively simple model has predictive power opens the door for further simulations in pursuit of greater understanding of the underlying molecular network. The same principles should apply to other molecular networks like the mammalian circadian clock and signaling pathways.

Both biological observations and the *cwo*-mutant model reveal that the *Drosophila* clock continues to oscillate with a 24-h period in LD in the absence of CWO, albeit with a change in amplitude. The question of the unique and essential contribution of CWO to the dynamics of the oscillating molecular circuit of the clock remains open.

SUPPORTING MATERIAL

Six figures, MATLAB functions, and one table are available at http://www.biophysj.org/biophysj/supplemental/S0006-3495(09)01376-9.

We are indebted to Michael Rosbash for sharing the *cry* microarray data and for very helpful discussions. We are also indebted to the referees whose suggestions directed us toward an exciting exploration.

REFERENCES

1. Allada, R., N. E. White, W. V. So, J. C. Hall, and M. Rosbash. 1998. A mutant *Drosophila* homolog of mammalian Clock disrupts circadian rhythms and transcription of *period* and *timeless*. *Cell*. 93:791–804.
2. Bae, K., C. Lee, D. Sidote, K. Y. Chuang, and I. Edery. 1998. Circadian regulation of a *Drosophila* homolog of the mammalian *Clock* gene: PER and TIM function as positive regulators. *Mol. Cell. Biol*. 18:6142–6151.
3. Darlington, T. K., K. Wager-Smith, M. F. Ceriani, D. Staknis, N. Gekakis, et al. 1998. Closing the circadian loop: CLOCK-induced transcription of its own inhibitors *per* and *tim*. *Science*. 280:1599–1603.
4. Hao, H., D. L. Allen, and P. E. Hardin. 1997. A circadian enhancer mediates PER-dependent mRNA cycling in *Drosophila melanogaster*. *Mol. Cell. Biol*. 17:3687–3693.
5. Rutila, J. E., V. Suri, M. Le, W. V. So, M. Rosbash, et al. 1998. CYCLE is a second bHLH-PAS clock protein essential for circadian rhythmicity and transcription of *Drosophila period* and *timeless*. *Cell*. 93:805–814.
6. McDonald, M. J., and M. Rosbash. 2001. Microarray analysis and organization of circadian gene expression in *Drosophila*. *Cell*. 107:567–578.
7. Honma, S., T. Kawamoto, Y. Takagi, K. Fujimoto, F. Sato, et al. 2002. *Dec1* and *dec2* are regulators of the mammalian molecular clock. *Nature*. 419:841–844.
8. Kadener, S., D. Stoleru, M. McDonald, P. Nawathean, and M. Rosbash. 2007. Clockwork orange is a transcriptional repressor and a new *Drosophila* circadian pacemaker component. *Genes Dev*. 21:1675–1686.
9. Matsumoto, A., M. Ukai-Tadenuma, R. G. Yamada, J. Houl, T. Kasukawa, et al. 2007. A functional genomics strategy reveals clockwork orange as a transcriptional regulator in the *Drosophila* circadian clock. *Genes Dev*. 21:1687–1700.
10. Richier, B., C. Michard-Vanhée, A. Lamouroux, C. Papin, and F. Rouyer. 2008. The clockwork orange *Drosophila* protein functions as both an activator and a repressor of clock gene expression. *J. Biol. Rhythms*. 23:103–116.
11. Lim, C., B. Y. Chung, J. L. Pitman, J. J. McGill, S. Pradhan, et al. 2007. Clockwork orange encodes a transcriptional repressor important for circadian-clock amplitude in *Drosophila*. *Curr. Biol*. 17:1082–1089.
12. Glossop, N. R., L. C. Lyons, and P. E. Hardin. 1999. Interlocked feedback loops within the *Drosophila* circadian oscillator. *Science*. 286:766–768.
13. Glossop, N. R., J. H. Houl, H. Zheng, F. S. Ng, S. M. Dudek, et al. 2003. VRILLE feeds back to control circadian transcription of *Clock* in the *Drosophila* circadian oscillator. *Neuron*. 37:249–261.
14. Blau, J., and M. W. Young. 1999. Cycling *vrille* expression is required for a functional *Drosophila* clock. *Cell*. 99:661–671.
15. Cyran, S. A., A. M. Buchsbaum, K. L. Reddy, M. C. Lin, N. R. Glossop, et al. 2003. *vrille*, *Pdp1*, and *dClock* form a second feedback loop in the *Drosophila* circadian clock. *Cell*. 112:329–341.
16. Smolen, P., P. E. Hardin, B. S. Lo, D. A. Baxter, and J. H. Byrne. 2004. Simulation of *Drosophila* circadian oscillations, mutations, and light responses by a model with VRI, PDP-1, and CLK. *Biophys. J*. 86:2786–2802.
17. Xie, Z., and D. Kulasiri. 2007. Modelling of circadian rhythms in *Drosophila* incorporating the interlocked PER/TIM and VRI/PDP1 feedback loops. *J. Theor. Biol*. 245:290–304.
18. Gekakis, N., L. Saez, A. M. Delahaye-Brown, M. P. Myers, A. Sehgal, et al. 1995. Isolation of timeless by PER protein interaction: defective interaction between timeless protein and long-period mutant PER_L. *Science*. 270:811–815.
19. Saez, L., and M. W. Young. 1996. Regulation of nuclear entry of the *Drosophila* clock proteins period and timeless. *Neuron*. 17:911–920.
20. Marrus, S. B., H. Zeng, and M. Rosbash. 1996. Effect of constant light and circadian entrainment of *per*S flies: evidence for light-mediated delay of the negative feedback loop in *Drosophila*. *EMBO J*. 15: 6877–6886.
21. Lee, C., K. Bae, and I. Edery. 1999. PER and TIM inhibit the DNA binding activity of a *Drosophila* CLOCK-CYC/dBMAL1 heterodimer without disrupting formation of the heterodimer: a basis for circadian transcription. *Mol. Cell. Biol*. 19:5316–5325.
22. Kloss, B., J. L. Price, L. Saez, J. Blau, A. Rothenfluh, et al. 1998. The *Drosophila* clock gene *double-time* encodes a protein closely related to human casein kinase Iε. *Cell*. 94:97–107.
23. Price, J. L., J. Blau, A. Rothenfluh, M. Abodeely, B. Kloss, et al. 1998. *double-time* is a novel *Drosophila* clock gene that regulates PERIOD protein accumulation. *Cell*. 94:83–95.
24. Yu, W., H. Zheng, J. H. Houl, B. Dauwalder, and P. E. Hardin. 2006. PER-dependent rhythms in CLK phosphorylation and E-box binding regulate circadian transcription. *Genes Dev*. 20:723–733.
25. Goldbeter, A. 1995. A model for circadian oscillations in the *Drosophila period* protein (PER). *Proc. Biol. Sci*. 261:319–324.
26. Leloup, J. C., and A. Goldbeter. 1998. A model for circadian rhythms in *Drosophila* incorporating the formation of a complex between the PER and TIM proteins. *J. Biol. Rhythms*. 13:70–87.
27. Smolen, P., D. A. Baxter, and J. H. Byrne. 2002. A reduced model clarifies the role of feedback loops and time delays in the *Drosophila* circadian oscillator. *Biophys. J*. 83:2349–2359.
28. Ueda, H. R., M. Hagiwara, and H. Kitano. 2001. Robust oscillations within the interlocked feedback model of *Drosophila* circadian rhythm. *J. Theor. Biol*. 210:401–406.
29. Dembinska, M. E., R. Stanewsky, J. C. Hall, and M. Rosbash. 2009. Circadian cycling of a PERIOD-β-galactosidase fusion protein in *Drosophila*: evidence for cyclical degradation. *J. Biol. Rhythms*. 12:157–172.
30. Hardin, P. E., J. C. Hall, and M. Rosbash. 1992. Circadian oscillations in *period* gene mRNA levels are transcriptionally regulated. *Proc. Natl. Acad. Sci. USA*. 89:11711–11715.
31. Price, J. L., M. E. Dembinska, M. W. Young, and M. Rosbash. 1995. Suppression of PERIOD protein abundance and circadian cycling by the *Drosophila* clock mutation timeless. *EMBO J*. 14:4044–4049.
32. Stanewsky, R., B. Frisch, C. Brandes, M. J. Hamblen-Coyle, M. Rosbash, et al. 1997. Temporal and spatial expression patterns of transgenes containing increasing amounts of the *Drosophila* clock gene period and a *lacZ* reporter: mapping elements of the PER protein involved in circadian cycling. *J. Neurosci*. 17:676–696.
33. Zuzak, T. J., D. F. Steinhoff, L. N. Sutton, P. C. Phillips, A. Eggert, et al. 2002. Loss of caspase-8 mRNA expression is common in childhood primitive neuroectodermal brain tumour/medulloblastoma. *Eur. J. Cancer*. 38:83–91.
34. Lee, C., K. Bae, and I. Edery. 1998. The *Drosophila* CLOCK protein undergoes daily rhythms in abundance, phosphorylation, and interactions with the PER-TIM complex. *Neuron*. 21:857–867.
35. Zeng, H., Z. Qian, M. P. Myers, and M. Rosbash. 1996. A light-entrainment mechanism for the *Drosophila* circadian clock. *Nature*. 380: 129–135.
36. Emery, P., W. V. So, M. Kaneko, J. C. Hall, and M. Rosbash. 1998. CRY, a *Drosophila* clock and light-regulated cryptochrome, is a major contributor to circadian rhythm resetting and photosensitivity. *Cell*. 95:669–679.
37. Chen, R., D. O. Seo, E. Bell, C. von Gall, and C. Lee. 2008. Strong resetting of the mammalian clock by constant light followed by constant darkness. *J. Neurosci*. 28:11839–11847.
38. Yu, Q., A. C. Jacquier, Y. Citri, M. Hamblen, J. C. Hall, et al. 1987. Molecular mapping of point mutations in the *period* gene that stop or speed up biological clocks in *Drosophila melanogaster*. *Proc. Natl. Acad. Sci. USA*. 84:784–788.
39. Konopka, R. J., and S. Benzer. 1971. Clock mutants of *Drosophila melanogaster*. *Proc. Natl. Acad. Sci. USA*. 68:2112–2116.
40. Kim, E. Y., H. W. Ko, W. Yu, P. E. Hardin, and I. Edery. 2007. A DOUBLETIME kinase binding domain on the *Drosophila* PERIOD protein is essential for its hyperphosphorylation, transcriptional repression, and circadian clock function. *Mol. Cell. Biol*. 27:5014–5028.

41. Kadener, S., J. S. Menet, R. Schoer, and M. Rosbash. 2008. Circadian transcription contributes to core period determination in *Drosophila*. *PLoS Biol*. 6:e119.

42. Bargiello, T. A., and M. W. Young. 1984. Molecular genetics of a biological clock in *Drosophila*. *Proc. Natl. Acad. Sci. USA*. 81:2142–2146.

43. Baylies, M. K., T. A. Bargiello, F. R. Jackson, and M. W. Young. 1987. Changes in abundance or structure of the *per* gene product can alter periodicity of the *Drosophila* clock. *Nature*. 326:390–392.

44. Smith, R. F., and R. J. Konopka. 1981. Circadian clock phenotypes of chromosome aberrations with a breakpoint at the *per* locus. *Mol. Gen. Genet*. 183:243–251.

45. Smith, R. F., and R. J. Konopka. 1982. Effects of dosage alterations at the *per* locus on the period of the circadian clock of *Drosophila*. *Mol. Gen. Genet*. 185:30–36.

46. Hardin, P. E., J. C. Hall, and M. Rosbash. 1990. Feedback of the *Drosophila period* gene product on circadian cycling of its messenger RNA levels. *Nature*. 343:536–540.

47. Van Gelder, R. N., and M. A. Krasnow. 1996. A novel circadianly expressed *Drosophila melanogaster* gene dependent on the *period* gene for its rhythmic expression. *EMBO J*. 15:1625–1631.

48. Sabouri-Ghomi, M., A. Ciliberto, S. Kar, B. Novak, and J. J. Tyson. 2008. Antagonism and bistability in protein interaction networks. *J. Theor. Biol*. 250:209–218.

49. Mjolsness, E., D. H. Sharp, and J. Reinitz. 2008. A connectionist model of development. *J. Theor. Biol*. 152:429–453.

50. Reinitz, J., E. Mjolsness, and D. H. Sharp. 1995. Model for cooperative control of positional information in *Drosophila* by bicoid and maternal hunchback. *J. Exp. Zool*. 27:47–56.

51. Reinitz, J., and D. H. Sharp. 1995. Mechanism of eve stripe formation. *Mech. Dev*. 49:133–158.

52. Sharp, D. H., and J. Reinitz. 1998. Prediction of mutant expression patterns using gene circuits. *Biosystems*. 47:79–90.

53. Reinitz, J., D. Kosman, C. E. Vanario-Alonso, and D. H. Sharp. 1998. Stripe forming architecture of the gap gene system. *Dev. Genet*. 23: 11–27.

54. Perkins, T. J., J. Jaeger, J. Reinitz, and L. Glass. 2006. Reverse engineering the gap gene network of *Drosophila melanogaster*. *PLOS Comput. Biol*. 2:417–428.

55. Jaeger, J., M. Blagov, D. Kosman, K. N. Kozlov, Manu, et al. 2004. Dynamical analysis of regulatory interactions in the gap gene system of *Drosophila melanogaster*. *Genetics*. 167:1721–1737.

56. Jaeger, J., S. Surkova, M. Blagov, H. Janssens, D. Kosman, et al. 2004. Dynamic control of positional information in the early *Drosophila* embryo. *Nature*. 430:368–371.

57. Leise, T. L., and E. E. Moin. 2007. A mathematical model of the *Drosophila* circadian clock with emphasis on posttranslational mechanisms. *J. Theor. Biol*. 248:48–63.

58. Yu, R. C., C. G. Pesce, A. Colman-Lerner, L. Lok, D. Pincus, et al. 2008. Negative feedback that improves information transmission in yeast signalling. *Nature*. 356:755–761.

59. Tsai, T. Y., Y. S. Choi, W. Ma, J. R. Pomerening, C. Tang, et al. 2008. Robust, tunable biological oscillations from interlinked positive and negative feedback loops. *Science*. 321:126–129.